(17) M. Eisenhut, H. L. Mitchell, D. D. Traficante, R. J. Kaufman, J. M. Deutsch, and G. M. Whitesides, *J. Am. Chem. Soc.*, **96**, 5385 (1974).
(18) R. G. Cavell, N. T. Yap, J. A. Gibson, L. Vande Griend, unpublished work.
(19) G. Binsch and D. L. Kleier, "DNMR3, A Computer Program for the Calculation of Exchange Broadened NMR Spectra", Program 165, Quantum Chemistry Program Exchange, Indiana University, Bloomington, Ind.
(20) This procedure is acceptable since there is a negligible chance of having two $^{13}CF_3$ groups in the same molecule in systems such as the present with natural-abundance carbon-13 nuclei.
(21) W. Klemperer, in "Dynamic NMR Spectroscopy", L. M. Jackman and F. A. Cotton, Ed., Academic Press, New York, N.Y., 1975.
(22) J. I. Musher, *J. Am. Chem. Soc.*, **94**, 5662 (1972).
(23) R. S. Berry, *J. Chem. Phys.*, **32**, 933 (1960).
(24) I. Ugi, D. Marquarding, H. Klusacek, P. Gillespie, and F. Ramirez, *Acc. Chem. Res.*, **4**, 288 (1971).
(25) A one-step BPR effects a trigonal-bipyramidal (TBP) to TBP rearrangement (via the square-pyramidal transition state or intermediate). In all cases considered herein, the product is a distinctly different isomer of the system in contrast to XPY_4 systems and the product isomer must return to an equilibrated, indistinguishably rearranged form of the initial isomer. Preserving the pivot and reverting by the reverse BPR process implies that the product has a short lifetime on the NMR time scale or the BPR process is instantaneous, but in either case axial–equatorial interchange does not result. Changing the pivot in the rearrangement implies the existence of a TBP intermediate with a sufficiently long lifetime for the species to "forget" the originally employed pivot and execute a second BPR with an arbitrarily chosen pivot achieving the desired equilibration.
(26) A locally adapted version of the program EXCHSYS described by J. K. Kreiger, J. M. Deutsch, and G. M. Whitesides, *Inorg. Chem.*, **12**, 1535 (1973). Details of the program are given in the thesis of J. K. Kreiger, MIT, Cambridge, Mass., 1971.
(27) K. Laidler, "Chemical Kinetics", McGraw-Hill, New York, N.Y., 1950.
(28) G. Binsch in "Dynamic Nuclear Magnetic Resonance Spectroscopy", L. M. Jackman and F. A. Cotton, Ed., Academic Press, New York, N.Y., 1975.
(29) Alternative analysis of the rate data assuming an intramolecular process with $\Delta S^* = 0$ and $A = 10^{13.2}$ yielded ΔH^* and E_a values which were within 0.5 kcal of each other. The resultant E_a values are within 1.0 kcal of and possess the same relative order as the ΔG^*_{298} values obtained by unconstrained least-squares analysis which are shown in Table III; thus the present comparisons based on ΔG^*_{298} are not altered of constrained intramolecular E_a values are used.
(30) J. M. Howell, *J. Am. Chem. Soc.*, **97**, 3930 (1975); F. Keil and W. Kutzelnigg, *ibid.*, **97**, 3623 (1975); J. M. Howell, J. R. Van Wazer, and A. R. Rossi, *Inorg. Chem.*, **13**, 1747 (1974).
(31) P. Gillespie, P. Hoffman, H. Klusacek, D. Marquarding, S. Pfohl, F. Ramirez, E. A.. Tsolis, and I. Ugi, *Angew. Chem., Int. Ed. Engl.*, **10**, 687 (1971).
(32) Clearly square-pyramidal isomers are also possible and may well be more stable than some of the trigonal-bipyramidal isomers considered.[2,3,30,31] In a complex system such as this one, the appropriate choice of structures is not clear; we make the simplifying assumptions that there is a "square pyramid" (regular or distorted) of higher energy[2] related to each of the TBP isomers shown which may be close to the transition-state geometry and that we can map a rearrangement through a series of isomers.
(33) A single ae permutation of the equatorial CH_3 group and the axial CF_3 group effects the A → D conversion and achieves equilibration in a single step, and while such a process may be possible, it cannot be either a BPR or TR mechanism which are cyclic permutations of the type aeae in which an axial *pair* is swapped for an equatorial pair by means of an appropriate motion. Thus D* is accessible from A by BPR whereas D is not. Similarly one-step equilibration would be achieved by direct A → C transformation, a transformation not available by means of a BPR or TR process.
(34) J. B. Stothers, "Carbon-13 Nuclear Magnetic Resonance Spectroscopy", Academic Press, New York, N.Y., 1972.
(35) T. C. Farrar and E. D. Becker, "Pulse and Fourier Transform NMR", Academic Press, New York, N.Y., 1971.

Contribution from the Department of Chemistry, Wayne State University, Detroit, Michigan 48202

Synthesis and Characterization of Several Novel Molybdenum Complexes of Cyclic Polythiaethers. Crystal and Molecular Structure of *sym*-Dihydrosulfido-bis(μ-1,5,9,13-tetrathiacyclohexadecane)-dimolybdenum(II) Trifluoromethanesulfonate Dihydrate

JOHN CRAGEL, JR., VIRGINIA B. PETT, MILTON D. GLICK, and RICHARD E. DESIMONE*

Received December 27, 1977

The reaction of $[Mo_2(CF_3SO_3)_2(H_2O)_4](CF_3SO_3)_2$ with the cyclic polythiaether 1,5,9,13-tetrathiacyclohexadecane yields several products, three of which have been extensively characterized. They are *sym*-dihydrosulfido-bis(μ-1,5,9,13-tetrathiacyclohexadecane)-dimolybdenum(II) trifluormethanesulfonate dihydrate (I), ethoxidooxobis(1,5,9,13-tetrathiacyclohexadecane)-μ-oxo-dimolybdenum(IV) trifluoromethanesulfonate hydrate (II), and hydrosulfido(1,5,9,13-tetrathiacyclohexadecane)oxomolybdenum(IV) trifluoromethanesulfonate (III). These are the first complexes in which molybdenum is coordinated by a macrocyclic ligand. I is a completely sulfur-coordinated sulfur-bridged binuclear species, II an oxo-bridged binuclear species, and III a monomer. UV–visible, IR, NMR, and cyclic voltammetric data are presented. Complex I crystallizes in the triclinic space group $P\bar{1}$ with one molecule per unit cell of dimensions $a = 10.827(2)$ Å, $b = 11.921(2)$ Å, $c = 9.234(1)$ Å, $\alpha = 97.22(1)°$, $\beta = 104.42(1)°$, $\gamma = 108.21(2)°$, and $V = 1069.5(4)$ Å^3. Full-matrix least-squares refinement gave final discrepancy factors of $R_1 = 0.040$ and $R_2 = 0.067$ for 2637 data having $F^2 > 2.5\sigma(F^2)$. The molecular structure is highlighted by the presence of a

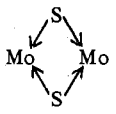

bridging unit with the bridging sulfurs each belonging to an intact macrocycle coordinated in the endo configuration. The Mo–Mo distance is 2.823 Å, and the metal–sulfur distances in the Mo coordination sphere imply that the bridge functions as a quite effective bonding unit. The other unique feature of this molecule is the presence of a terminal –SH group on each Mo atom, the first reported example of such an anion on a Mo^{II} complex.

Introduction

Complexes of macrocyclic ligands have in recent years received attention from an increasingly large share of inorganic chemists. Much of this attention has been devoted to nitrogen-containing macrocycles which have the obvious feature of serving as (sometimes) useful models for naturally occurring macrocyclic species.[1-5] More recently, oxygen-containing macrocycles—the "crown ethers" and the bicyclic cryptates—have also been the focus of considerable interest, again mainly from a biological viewpoint.[6-8] Large cyclic molecules containing sulfur as the heteroatom have received less attention than probably any class of macrocyclic species,[9-13] although their potential utility in several areas should not be underestimated. We have been involved in a program of synthesis

0020-1669/78/1317-2885$01.00/0

and characterization of metal complexes of the cyclic polythiaethers with a number of transition metals. In particular we have focused attention on the chemistry of the early second- and third-row transition metals, Nb, Mo, and W.

Among the reasons for undertaking this work is the current demand for knowledge of molybdenum chemistry in view of the relevance of that metal to biological problems.[14-16] We have taken the approach of studying fundamental chemistry which will shed light on the nature of the complexes formed between molybdenum and sulfur-containing molecules, rather than that of simple "model building". We hope that the complexes produced will have some value to those more deeply involved in the study of biological molybdenum.

Our initial studies involved complexes of the high-oxidation-state metal halides and oxyhalides of Mo, Nb, and W with a variety of cyclic polythiaethers of general formula[17]

$$\underbrace{-\{(CH_2)_n-S(CH_2)_m-S\}_l-}$$

$l = 2\text{-}4$
$n = 2\text{-}5$
$m = 2\text{-}5$

The chemistry of the complexes so formed is exceedingly sparse and difficult.[18,19] As might be expected for relatively soft ligands and hard metals, the interactions are quite weak and the complexes very unstable. All complexes formed by direct interaction of metal halide (or oxohalide) and ligand in "inert" solvents are of a simple acid–base nature, involve no displacement of halide ions, and involve coordination of only one sulfur atom per metal. The complexes tend to decompose in any solvent in which they are soluble, thus precluding any solution chemistry. In addition, the extreme air and/or moisture sensitivity further limits characterization. Among the number of complexes produced, the molecule $(NbCl_5)_2$14-ane$[S_4]$ was characterized by X-ray crystallography[20] and serves as a prototype for other molecules of this type. The dominant structural feature is the *exo*- or inside-out conformation of the macrocycle, which had not previously been observed. Subsequent investigation showed the free ligand to have the same conformation.[21]

More recently we have approached the synthesis of complexes from the lower oxidation-state compounds of molybdenum and have met with considerably greater success. This paper will concern itself with the reaction of "tetrakis(trifluoromethanesulfonato)dimolybdenum(II)"[22] and the 16-membered S_4 macrocycle 16-ane$[S_4]$,[23] the characterization of the reaction products, and the crystal and molecular structure of the major product.

Experimental Section

Materials Trifluoromethanesulfonic acid was dried over molecular sieves (4-Å) and degassed by freeze thawing on the vacuum line in a Teflon-sealed container. It was transferred, in the container, to the glovebox and used without further purification. $Mo_2(O_2CH)_4$ was prepared from the acetate using the method of Cotton.[24] Absolute ethanol, used in all preparations, was dried by refluxing over magnesium turnings followed by distillation under argon. It was bottled, sealed under a rubber septum, and transferred to the glovebox where it was degassed for 30 min with argon. At no time did the ethanol come in contact with air during drying or transfer. CH_3CN for spectral measurements was distilled from P_2O_5 and stored over 4-Å molecular sieves. For electrochemical measurements drying over sieves was repeated after the supporting electrolyte had been added. CD_3CN and $CDCl_3$ were obtained from NMR Specialties, Inc.

Reaction of $Mo_2(O_2CH)_4$ with CF_3SO_3H and 16-ane$[S_4]$. Trifluoromethanesulfonic acid (2 mL) and $Mo_2(O_2CH)_4$ (0.37 g, 0.001 mol) were combined under argon in a small ⅋ 19/38 flask (~10 mL volume), fitted with a microdistillation head, and heated with stirring to 70 °C. A gas (presumably CO) was evolved, and after 20 min, all of the yellow $Mo_2(O_2CH)_4$ had dissolved yielding a deep wine red solution. Heating was continued for a total of 40 min. After cooling to room temperature, the solution was vacuum distilled (at about 90 °C) to dryness. Cooling of the solution is necessary prior to distillation to avoid excessive bumping. After distillation the ⅋ 19/38 container was transferred to a drying pistol and dried at 110 °C (boiling toluene) and $\sim 10^{-5}$ Torr for a minimum of 48 h. During this time the color of the solid changed from deep red to a light pink. The drying pistol was then returned to the glovebox, and the solid was slowly added with stirring to 20 mL of absolute ethanol containing 16-ane$[S_4]$ (0.59 g, 0.002 mol). An extra 10 mL of absolute ethanol was used to quantitatively wash all "$Mo_2(TFMS)_4$" from the ⅋ 19/38 container. The combined mixture was then heated to 70 °C for 30 min, covered, and cooled to room temperature overnight. An orange solid, I, forms on cooling. This can be recrystallized from a minimum of hot absolute ethanol or acetonitrile.

The filtrate, after removal of the yellow solid, was further evaporated under argon and allowed to stand at room temperature. From this solution a blue product, II, slowly precipitated over a period of about 48 h. It was filtered and vacuum dried. A third crystalline product, III, red-brown, was isolated after several weeks from this same filtrate.

All products were soluble in CH_3CN, and the blue product was also soluble in H_2O. I decomposed at 237–243 °C, II decomposed at 149–154 °C and III decomposed at 230–235 °C.

Characterization of Complexes. IR spectra were recorded as Nujol mulls or KBr pellets on a Perkin-Elmer 621 spectrometer.

^{13}C NMR spectra were recorded on a Jeolco FX-60 spectrometer in 10-mm sample tubes in CD_3CN and $CDCl_3$.

Optical spectra were recorded in CH_3CN solution on a Cary-14 spectrophotometer.

CV spectra were recorded on a conventional operational amplifier-based electrochemical instrument which includes a three-electrode controller, a precise triangular wave generator, and current-follower for cell current measurements. Solvent was CH_3CN, supporting electrolyte was $(CH_3)_4NClO_4$, and concentrations were 10^{-3}–10^{-4} M. Platinum working and auxillary electrodes were used. An aqueous saturated calomel standard electrode served as reference.

Collection of X-ray Data. A suitable crystal of I, grown from hot CH_3CN, and measuring approximately 0.12 × 0.15 × 0.30 mm, was sealed in a thin-walled capillary and mounted on a Syntex $P2_1$ diffractometer. Oscillation photographs and a small set of counter data established that the crystal was triclinic. Fifteen reflections with 2θ between 18 and 34° were centered using a programmed centering routine. Lattice constants and errors were determined by least-squares refinement of the angles defining these 15 reflections, yielding the values a = 13.370 (3) Å, b = 21.154 (2) Å, c = 18.939 (2) Å, α = 88.53 (1)°, β = 89.86 (2)°, and γ = 87.19 (1)° and giving a cell volume of 5348.2 ± 1.5 Å. Data collection proceeded with these cell parameters. Intensity data were collected to a value of 2θ = 45° in the $h\pm k\pm l$ quadrants using Mo Kα radiation (λ = 0.710 69 Å) at ~20 °C. The monochromator consisted of a highly oriented graphite crystal in the parallel mode. The θ–2θ scan technique was used with a scan rate of 2.02°/min. Backgrounds were measured at each end of the scan for a total time equal to half the scan time. During data collection, the intensities of three standard reflections were measured every 50 reflections with no indication of decomposition or crystal movement. The data were reduced to F^2 and $\sigma(F^2)$ by procedures previously described.[25a] Standard deviations were assigned as

$$\sigma(I) = [\sigma_{\text{counter}}(I^2) + (0.04I)^2]^{1/2}$$

where $\sigma_{\text{counter}} = (1 + K^2B)^{1/2}$, I = net intensity, B = total background counts, and K = ratio of scan time to background time. Extinction and absorption corrections were not applied. The linear absorption coefficient for Mo Kα radiation is μ = 12.0 cm^{-1}. Corrections were made for both real and imaginary parts of the anomalous dispersion factor.[25b] Data for which $F^2 > 2.5\sigma(F^2)$ were separated from the entire data set of over 16 000 collected reflections. Approximately one in every five reflections was observed. A thorough examination of the data revealed that an unconventional cell had been chosen such that the observed reflections were given by $2h + 2k - l = 5n$, n = integer. Plotting reciprocal lattice points enabled the transformation to a new smaller cell to be made; the required transformation is

$$\begin{bmatrix} -2 & 0 & 1 \\ -1 & 1 & 0 \\ 1 & 0 & 2 \end{bmatrix} \begin{bmatrix} a^* \\ b^* \\ c^* \end{bmatrix} = \begin{bmatrix} (a^*)' \\ (b^*)' \\ (c^*)' \end{bmatrix}$$

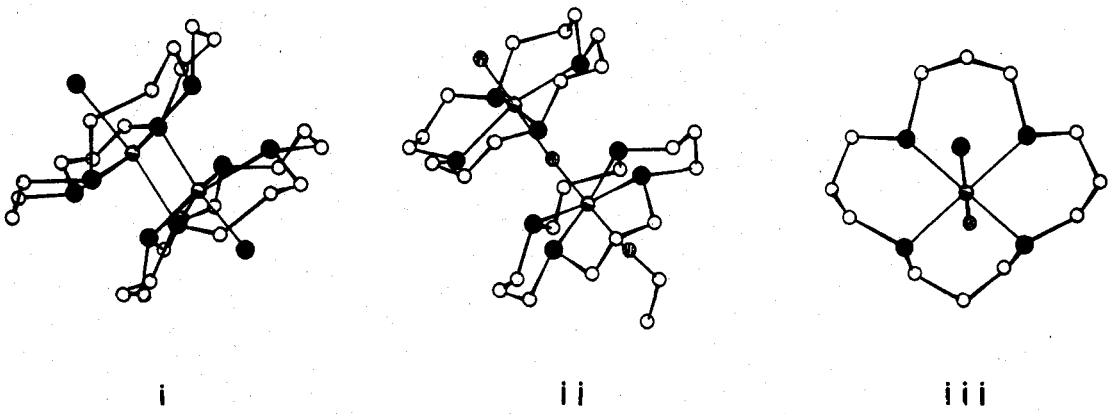

i ii iii

Figure 1. Characterized products described in this study (cations only): (I) *sym*-dihydrosulfido-bis(μ-1,5,9,13-tetrathiacyclohexadecane)-dimolybdenum(II) trifluoromethanesulfonate dihydrate, (II) ethoxidooxobis(1,5,9,13-tetrathiacyclohexadecane-μ-oxo-dimolybdenum(IV) trifluoromethanesulfonate hydrate, (III) hydrosulfido(1,5,9,13-tetrathiacyclohexadecane)oxomolybdenum(IV) trifluoromethanesulfonate; ○ = C, ● = S, ◎ = O, ◐ = Mo.

The inverse transpose of the matrix gives the transformation to the direct cell axes. The program TRACER was then applied to generate lattice constants for the new primitive triclinic cell in the conventional orientation. A repetition of the autoindexing and least-squares routines used by the Syntex $P2_1$ system gave refined lattice constants along with standard deviations. These are $a = 10.8274 \pm 0.0023$ Å, $b = 11.9215 \pm 0.0022$ Å, $c = 9.2349 \pm 0.0013$ Å, $\alpha = 97.221 \pm 0.013°$, $\beta = 104.424 \pm 0.014°$, $\gamma = 108.206 \pm 0.017°$, and $V = 1069.49 \pm 0.36$ Å^3. Using this calculated volume, the calculated density based on one molecule per unit cell is 1.84 g/cm^3; the experimental value is also 1.84 g/cm^3.

The transformation relating direct axes was used to convert Miller indices. Of 2751 observed reflections, 114 low-intensity reflections transformed to noninteger indices and were eliminated from the data set. These reflections appeared completely random. The final data set consisted of 2637 reflections. As a final check on the new data set, it was confirmed that all vectors present in the Patterson map of the new cell were also present in the original cell.

Owing to some uncertainty involving the nature of the dimeric unit (we expected a quadruply bonded Mo_2^{4+} species) the correct solution to the Patterson map was not immediately obvious. Iterative application of the Sayre relationship for centrosymmetric crystals using 374 reflections with $E > 1.3$ yielded a solution consistent with the Patterson synthesis and led to the correct location of the molybdenum atom in a $P\bar{1}$ cell. Atomic positions of the sulfur atoms were located immediately from a Fourier map phased by molybdenum alone. The nature of the bridging unit and the existence of the terminal sulfur became obvious at this point. Inclusion of the remaining nonhydrogen atoms, together with refinement of positional and isotropic thermal parameters, produced a standard unweighted residual $R_1 = (\sum||F_o| - |F_c||)/\sum|F_o|$ of 0.090. Addition of calculated hydrogen atom structure factors for all hydrogen atoms except the hydrogen atom on the terminal sulfur lowered R to 0.078. (A total of 20 of 24 hydrogen atoms were located on the difference map, but calculated positions were used.) Anisotropic refinement on the Mo and S atoms yielded $R = 0.045$. Anisotropic refinement on all nonhydrogen atoms, with a total of 244 variables, resulted in a final unweighted R_1 of 0.040 and a weighted $R_2 = [(\sum w(|F_o| - |F_c|)^2)/\sum wF_o^2]^{1/2}$ of 0.067. A final difference Fourier map showed the highest residual peak (1.03 e) to be within the anion. The highest residual peak in the cation is 0.57 e/Å^3 at 0.54 Å from S(5), the terminal sulfur.

Results and Discussion

In carrying out these reactions, it was our intent to find a material which decomposes cleanly and easily leaving an Mo_2^{4+} species which would then readily coordinate with the weakly coordinating thiaether. The trifluoromethanesulfonate complex, "$Mo_2(TFMS)_4$", seemed to satisfy that requirement in that the acid is extremely strong and the anion correspondingly weak. Previous attempts with carboxylate and sulfate species proved unsuccessful.[26] The complex $Mo_2(O_2CH)_4$ is preferred to other carboxylates since in acid

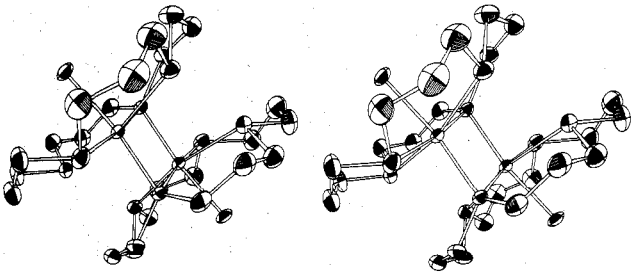

Figure 2. Stereoscopic view of the cation of I. Thermal ellipsoids are shown to enclose 50% probability.

solution decomposition proceeds readily with evolution of CO and H_2O according to the equation

$$Mo_2(O_2CH)_4 + 4CF_3SO_3H \rightarrow \text{“}Mo_2(CF_3SO_3)_4\text{”} + 4H_2O + 4CO \quad (1)$$

In this reaction the product "$Mo_2(CF_3SO_3)_4$" has been shown to be $[Mo_2(H_2O)_4(CF_3SO_3)_2](CF_3SO_3)_2$ due to the presence of evolved H_2O.[22] Coordinated water can be avoided by using acetate, for example, but then it becomes exceedingly difficult to remove traces of acetate which remain.

The reaction of "$Mo_2(TFMS)_4$" with 16-ane[S_4] is complex and yields multiple products (eq 2 and Figure 1). The nature

$$\text{“}Mo_2(CF_3SO_3)_4\text{”} + \text{16-ane}[S_4] \xrightarrow[\text{EtOH}]{} [Mo_2^{II}(SH)_2(\text{16-ane}[S_4])_2](CF_3SO_3)_2\cdot 2H_2O + [Mo_2^{IV}O_2(\text{16-ane}[S_4])_2OC_2H_5](CF_3SO_3)_3\cdot H_2O + [Mo^{IV}O(SH)\text{16-ane}[S_4]]CF_3SO_3 \quad (2)$$

of the products implies that the solvent plays an active role and that some of the ligand is cleaved during the reaction. The principal product is I, $[Mo_2^{II}(SH)_2(\text{16-ane}[S_4])_2](CF_3SO_3)_2\cdot 2H_2O$. This compound has the structure shown in Figure 1(i). The secondary products of the reaction, II, $[Mo_2^{IV}O_2(\text{16-ane}[S_4])_2OC_2H_5](CF_3SO_3)_3\cdot H_2O$, and III, $[Mo^{IV}O(SH)\text{16-ane}[S_4]]CF_3SO_3$, have structures as shown in Figure 1(ii), (iii), respectively. From these structures one sees (a) that the quadruple bond no longer exists in any of these molecules, (b) that solvent is involved at some point in the reaction, at least for II and possibly III, and (c) that a certain amount of macrocycle decomposition occurs, generating the –SH anion coordinated to I and III. Each of the complexes I–III will be discussed in detail below.

$[Mo_2^{II}(SH)_2(\text{16-ane}[S_4])_2](CF_3SO_3)_2\cdot 2H_2O$ (I). This complex is indefinitely stable in the solid state and in CH_3CN solution. The structure of the cation $[Mo_2(SH)_2(\text{16-ane}[S_4])]^{+2}$ is shown in stereoscopic projection in Figure 2, and

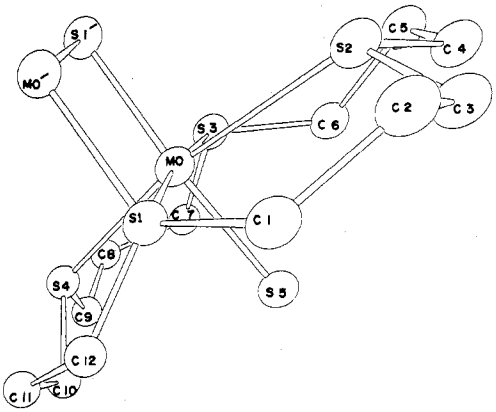

Figure 3. Atom-labeling scheme for the asymmetric unit of the cation of I.

the atom labelling scheme for the asymmetric unit is shown in Figure 3. The quadruple metal–metal bond present in the starting material has been replaced by the bridging

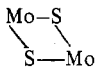

unit giving rise to an offset-stacked structure where the entire coordination sphere about the metal is composed of sulfur atoms: four nonbridging and one bridging sulfur from the macrocycle and a terminal –SH group. As required by the space group $P\bar{1}$, the single binuclear molecule in the unit cell possesses a center of inversion located between the two molybdenum atoms. Table I lists atomic coordinates and thermal parameters with standard deviations for nonhydrogen atoms in the asymmetric unit, and Table II lists significant bond lengths and angles. As an aid to visualizing the ring conformation, a schematic drawing of the cation is presented in Figure 4. A tabulation of dihedral angles and displacements from the plane of the four sulfur atoms of the macrocycle is given in Table III. A listing of calculated and observed structure factors and a figure showing the unit cell contents in stereoscopic projection are available.[27]

The metal coordination sphere is highlighted by two one-atom bridges which appear unique among Mo^{II} complexes so far structurally characterized. The two Mo atoms are 2.823 Å apart, a distance for which significant metal–metal interaction is certainly possible and which is commonly found in disulfido-bridged molybdenum(V) complexes.[28-32] As a result of the confining influence of the bridge, each Mo atom sits ~0.2 Å out of the plane defined by the four sulfurs of the macrocycle and is displaced toward the inversion center. As a further consequence of the bridging structure, the metal atom placement within the macrocycle cavity is quite "off-center". The Mo–S(1) distance, defining one bridge, is only 2.320 Å. This is quite a significant shortening compared to other nonbridging distances. The Mo–S(3) distance to the sulfur trans to the bridging sulfur is relatively long, 2.537 Å. The extra shortening of the Mo–S(1) bond may result from an additional "pulling" of that sulfur out of its normal position to accommodate the requirements of the bridges. The effect of this is seen in Figure 4 where it may be noted that the part of the ring around S(1) is pulled considerably away from its normal position, toward the plane defined by the four sulfur atoms of the ring. The Mo–S′(1) distance, which defines the other bridge, is also short, measuring 2.380 Å.

From these relatively short distances, and the accompanying ring distortion, it may be inferred that this bridging structure is quite an effective bonding unit. In view of the fact that it has replaced the strong Mo–Mo quadruple bond, the bridge seems of necessity to be moderately strong. This is not to say,

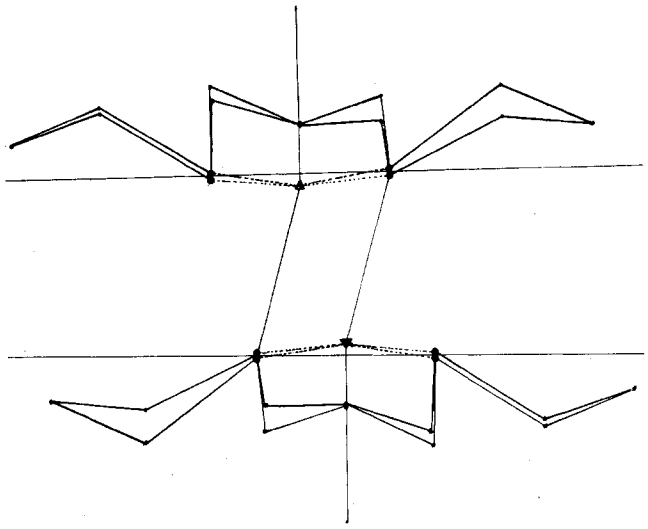

Figure 4. Schematic drawing of the cation of I showing ring conformation and location of metal ion relative to the ring: ● = S, ▲ = Mo.

however, that since we went from a quadruply bonded to a bridged structure, the sulfur bridge must be a stronger unit. Since nothing is known of the mechanism of the reaction, the apparent improbability of the quadruple bond to bridge transformation should not prejudice judgments of bond strength.

The other significant feature of the metal coordination sphere is the presence of the terminal –SH group. The identity of this group is established on several grounds, although it is not conclusively proved by any single piece of evidence. Since the reaction mixture leading to the complex contained sulfur only in the macrocycle, one must conclude that some decomposition of the macrocycle has occurred. This is not unreasonable since the dimolybdenum trifluoromethanesulfonate was "dried" of excess acid by prolonged pumping under high vacuum. Any small amount of residual acid trapped in the solid could have led to cleavage of the ring,[33] if only for a fraction of the total macrocycle present. One might have expected –S–R and R–S–R fragments to have been produced during ring cleavage, but there is absolutely no trace of alkyl fragments to be found and one must conclude that only a single sulfur (or –SH) is coordinated to Mo. We have discounted the possibility of Cl^- being the anion, even though it would appear in the electron density map very similar to S, since no Cl was contained in *any* of the reactants or their precursors. As pointed out in the Experimental Section, the largest residual peak in the final difference Fourier map is located ~0.5 Å from S(5) and is equivalent to 0.57 e. While this does not, in our opinion, of itself qualify as the "lost" H atom, when combined with the relatively anisotropic thermal ellipsoid of S(5), and the Mo–S(5)–"H" angle of 130°, it tends to make one suspect that something is there but unresolved due to the relatively large amount of electron density associated with the sulfur. Attempts to refine the parameters of this "peak" were unsuccessful. After a few cycles the electron density merged with that of S(5).

If we accept the fact that a lone sulfur atom occupies the sixth coordination site of the Mo atom, the question arises as to the Mo–S bond order and the oxidation state of the metal. Mo=S would require Mo^{III}; Mo—SH would require Mo^{II}. The Mo–S(5) bond length is 2.471 Å and the complex is diamagnetic. The observed diamagnetism could be due to a strong spin-pairing of $S = 1$ Mo^{II} or $S = {}^1/_2$ Mo^{III} ions, or to uncoupled and very distorted diamagnetic Mo^{II}. We hope future experiments will answer the question of the existence and extent of metal–metal interaction, but at this time we favor

Table I. Atomic Coordinates and Thermal Parameters[a-c]

atom	x	y	z	β_{11}	β_{22}	β_{33}	β_{12}	β_{13}	β_{23}
Mo	0.48650 (5)	0.58076 (4)	0.40292 (5)	0.00489 (7)	0.00370 (6)	0.00448 (9)	0.00164 (5)	0.00171 (5)	0.00130 (4)
S(1)	0.5348 (1)	0.4070 (1)	0.3458 (2)	0.0054 (2)	0.0038 (1)	0.0050 (2)	0.0019 (1)	0.0021 (1)	0.0009 (1)
S(2)	0.7342 (2)	0.7029 (1)	0.4810 (2)	0.0058 (2)	0.0047 (1)	0.0075 (2)	0.0009 (1)	0.0022 (2)	0.0015 (1)
S(3)	0.4366 (2)	0.7750 (1)	0.4377 (2)	0.0093 (2)	0.0049 (1)	0.0088 (2)	0.0034 (1)	0.0038 (2)	0.0026 (1)
S(4)	0.2436 (2)	0.4637 (1)	0.2677 (2)	0.0054 (2)	0.0059 (1)	0.0065 (2)	0.0021 (1)	0.0008 (1)	0.0017 (1)
S(5)	0.4938 (2)	0.6183 (1)	0.1475 (2)	0.0090 (2)	0.0059 (1)	0.0048 (2)	0.0027 (1)	0.0032 (2)	0.0024 (1)
S(6)	0.8791 (2)	0.1855 (2)	0.1921 (2)	0.0078 (2)	0.0080 (2)	0.0177 (4)	0.0022 (2)	0.0031 (2)	0.0006 (2)
C(1)	0.6911 (7)	0.4112 (6)	0.3010 (7)	0.0089 (9)	0.0070 (6)	0.0107 (10)	0.0034 (6)	0.0068 (8)	0.0008 (6)
C(2)	0.8222 (6)	0.5180 (6)	0.3850 (8)	0.0064 (8)	0.0082 (7)	0.0111 (10)	0.0030 (6)	0.0038 (7)	0.0019 (7)
C(3)	0.8200 (7)	0.6413 (6)	0.3618 (8)	0.0080 (8)	0.0069 (6)	0.0120 (11)	0.0025 (6)	0.0052 (8)	0.0018 (7)
C(4)	0.7781 (7)	0.8511 (6)	0.4319 (9)	0.0099 (9)	0.0045 (6)	0.0163 (12)	0.0004 (6)	0.0053 (9)	0.0030 (7)
C(5)	0.7030 (8)	0.9277 (6)	0.4854 (9)	0.0139 (11)	0.0045 (6)	0.0158 (13)	0.0017 (6)	0.0057 (9)	0.0025 (7)
C(6)	0.5583 (8)	0.8941 (6)	0.3847 (8)	0.0120 (10)	0.0049 (6)	0.0137 (11)	0.0021 (6)	0.0047 (9)	0.0036 (7)
C(7)	0.2871 (8)	0.7696 (6)	0.2883 (9)	0.0106 (10)	0.0073 (7)	0.0146 (12)	0.0051 (7)	0.0019 (9)	0.0044 (7)
C(8)	0.1587 (7)	0.6630 (7)	0.2715 (8)	0.0083 (9)	0.0105 (8)	0.0149 (12)	0.0063 (7)	0.0024 (8)	0.0049 (8)
C(9)	0.1473 (7)	0.5469 (7)	0.1701 (8)	0.0085 (9)	0.0085 (7)	0.0106 (11)	0.0046 (7)	0.0003 (8)	0.0030 (7)
C(10)	0.2269 (7)	0.3556 (6)	0.1015 (7)	0.0093 (9)	0.0066 (6)	0.0059 (8)	0.0026 (6)	−0.0001 (7)	−0.0004 (6)
C(11)	0.2711 (7)	0.2519 (6)	0.1423 (7)	0.0080 (8)	0.0059 (6)	0.0083 (9)	0.0011 (6)	0.0024 (7)	−0.0004 (6)
C(12)	0.4242 (7)	0.2790 (6)	0.1862 (7)	0.0084 (8)	0.0054 (6)	0.0055 (8)	0.0012 (5)	0.0020 (6)	−0.0009 (5)
C(13)	0.7082 (8)	0.0818 (7)	0.0940 (10)	0.0099 (10)	0.0094 (8)	0.0166 (14)	0.0024 (7)	0.0023 (10)	0.0070 (9)
O(1)	0.9629 (7)	0.1268 (7)	0.1566 (12)	0.0123 (9)	0.0164 (10)	0.0524 (24)	0.0071 (8)	0.0070 (12)	−0.0023 (12)
O(2)	0.8821 (8)	0.2913 (6)	0.1303 (11)	0.0187 (11)	0.0085 (7)	0.0492 (24)	−0.0001 (6)	0.0066 (13)	0.0072 (10)
O(3)	0.8763 (8)	0.2027 (9)	0.3452 (9)	0.0203 (12)	0.0273 (15)	0.0193 (13)	0.0028 (10)	0.0008 (10)	−0.0027 (11)
O(4)	0.0251 (7)	0.9037 (7)	0.1825 (8)	0.0200 (11)	0.0156 (9)	0.0244 (13)	0.0085 (8)	0.0022 (9)	0.0026 (9)
F(1)	0.6873 (6)	−0.0282 (5)	0.1222 (7)	0.0204 (9)	0.0113 (6)	0.0243 (10)	0.0003 (6)	0.0077 (8)	0.0055 (6)
F(2)	0.6181 (6)	0.1163 (7)	0.1105 (13)	0.0083 (7)	0.0172 (9)	0.0996 (39)	0.0043 (6)	0.0050 (12)	−0.212 (15)
F(3)	0.6903 (7)	0.0498 (6)	−0.0584 (7)	0.0269 (12)	0.0157 (8)	0.0230 (12)	−0.0024 (7)	−0.0013 (9)	0.0069 (8)

atom	x	y	z	atom	x	y	z
H(1)	0.6722	0.4040	0.1828	H(13)	0.3092	0.7584	0.1735
H(2)	0.7106	0.3313	0.3338	H(14)	0.2670	0.8508	0.3030
H(3)	0.9022	0.5031	0.3425	H(15)	0.0711	0.6860	0.2149
H(4)	0.8476	0.5217	0.5057	H(16)	0.1586	0.6500	0.3801
H(5)	0.9240	0.7039	0.3891	H(17)	0.0385	0.4897	0.1350
H(6)	0.7671	0.6332	0.2420	H(18)	0.1774	0.5667	0.0740
H(7)	0.7514	0.8377	0.3086	H(19)	0.2868	0.4006	0.0356
H(8)	0.8870	0.8983	0.4817	H(20)	0.1202	0.3160	0.0332
H(9)	0.7628	1.0216	0.4962	H(21)	0.2253	0.1765	0.0419
H(10)	0.7016	0.9150	0.6017	H(22)	0.2379	0.2240	0.2355
H(11)	0.5299	0.9733	0.3879	H(23)	0.4424	0.1995	0.2157
H(12)	0.5542	0.8618	0.2650	H(24)	0.4567	0.2966	0.0867

[a] Standard deviations from the full variance covariance matrix are given in parentheses for the least significant digit(s). [b] The form of the anisotropic temperature factor is $\exp[-(h^2\beta_{11} + k^2\beta_{22} + l^2\beta_{33} + 2hk\beta_{12} + 2hl\beta_{13} + 2kl\beta_{23})]$. [c] Calculated H atom positions. H atom $B = 5.0$.

Table II.[a] Interatomic Distances (Å) and Angles (deg)

Mo-S(1)	2.320 (1)	C(1)-C(2)	1.520 (9)
Mo-S(2)	2.483 (2)	C(2)-C(3)	1.518 (10)
Mo-S(3)	2.537 (2)	C(4)-C(5)	1.513 (10)
Mo-S(4)	2.461 (2)	C(5)-C(6)	1.506 (11)
Mo-S(5)	2.471 (2)	C(7)-C(8)	1.520 (11)
Mo-Mo'	2.823 (1)	C(8)-C(9)	1.523 (10)
Mo-S'(1)	2.380 (1)	C(10)-C(11)	1.515 (9)
S(1)-S'(1)	3.759 (3)	C(11)-C(12)	1.521 (9)
S(5)-S'(5)	3.726 (3)	S(6)-C(13)	1.796 (8)
S(1)-C(1)	1.826 (6)	S(6)-O(1)	1.381 (7)
S(1)-C(12)	1.830 (6)	S(6)-O(2)	1.413 (8)
S(2)-C(3)	1.827 (7)	S(6)-O(3)	1.443 (8)
S(2)-C(4)	1.830 (7)	C(13)-F(1)	1.205 (10)
S(3)-C(6)	1.822 (7)	C(13)-F(2)	1.330 (9)
S(3)-C(7)	1.825 (7)	C(13)-F(3)	1.360 (10)
S(4)-C(9)	1.808 (6)		
S(4)-C(10)	1.812 (6)		

S(5)-Mo-S(1)	89.31 (5)	C(4)-C(5)-C(6)	114.1 (6)
S(5)-Mo-S(2)	83.40 (5)	C(5)-C(6)-S(3)	112.8 (5)
S(5)-Mo-S(3)	84.52 (5)	S(3)-C(7)-C(8)	113.7 (5)
S(5)-Mo-S(4)	83.86 (5)	C(7)-C(8)-C(9)	113.4 (6)
S(1)-Mo-S(2)	89.54 (6)	C(8)-C(9)-S(4)	114.0 (5)
S(1)-Mo-S(3)	173.81 (5)	S(4)-C(10)-C(11)	113.1 (4)
S(2)-Mo-S(3)	89.32 (6)	C(10)-C(11)-C(12)	115.2 (6)
S(2)-Mo-S(4)	167.20 (7)	C(11)-C(12)-S(1)	117.8 (4)
S(3)-Mo-S(4)	90.75 (6)	O(1)-S(6)-O(2)	117.1 (6)
S(4)-Mo-S(1)	89.01 (5)	O(1)-S(6)-O(3)	116.3 (6)
C(12)-S(1)-C(1)	94.1 (3)	O(2)-S(6)-O(3)	112.0 (5)
C(3)-S(2)-C(4)	95.5 (3)	O(1)-S(6)-C(13)	105.2 (4)
		O(2)-S(6)-C(13)	102.5 (4)
C(6)-S(3)-C(7)	95.3 (3)	O(3)-S(6)-C(13)	101.0 (5)
C(9)-S(4)-C(10)	98.2 (3)	F(1)-C(13)-F(2)	110.7 (8)
S(1)-C(1)-C(2)	118.6 (4)	F(1)-C(13)-F(3)	96.8 (7)
C(1)-C(2)-C(3)	115.7 (5)	F(2)-C(13)-F(3)	108.8 (8)
C(2)-C(3)-S(2)	112.7 (5)	F(1)-C(13)-S(6)	112.6 (5)
S(2)-C(4)-C(5)	113.6 (5)	F(2)-C(13)-S(6)	115.8 (7)
		F(3)-C(13)-S(6)	110.5 (6)

[a] Number in parentheses represents the estimated standard deviation of the least significant digit(s). [b] Prime refers to symmetry atoms related by the inversion center.

Table III

dihedral angle[a]		displacement[b] from plane	
(C(10)-S(1)-C(1)-C(2))	−170	S(1)	0.07
(S(1)-C(1)-C(2)-C(3))	165	C(1)	−0.72
(C(1)-C(2)-C(3)-S(2))	−57	C(2)	−0.66
(C(2)-C(3)-S(2)-C(4))	81	C(3)	−1.23
(C(3)-S(2)-C(4)-C(5))	167	S(2)	−0.07
(S(2)-C(4)-C(5)-C(6))	169	C(4)	−0.97
(C(4)-C(5)-C(6)-S(3))	−82	C(5)	−0.41
(C(5)-C(6)-S(3)-C(7))	84	C(6)	−0.90
(C(6)-S(3)-C(7)-C(8))	−169	S(3)	0.07
(S(3)-C(7)-C(8)-C(9))	179	C(7)	−1.08
(C(7)-C(8)-C(9)-S(4))	−87	C(8)	−0.62
(C(8)-C(9)-S(4)-C(10))	79	C(9)	−1.07
(C(9)-S(4)-C(10)-C(11))	−169	S(4)	−0.07
(S(4)-C(10)-C(11)-C(12))	−173	C(10)	−1.20
(C10)-C(11)-C(12)-S(1))	−80	C(11)	−0.6
(C(11)-C(12)-S(1)-C(1))	61	C(12)	−0.74

[a] (a, b, c, d) denotes the dihedral angle (in degrees) between planes defined by (a, b, c) and (b, c, d). [b] Atomic displacement (in Å) from the mean plane through S(1), S(2), S(3), and S(4).

the Mo^{II} assignment. A Mo=S bond would be expected to be considerably shorter than that observed. One recently observed Mo^{V}=S terminal bond distance was found to be as short as 1.937 Å;[28] a series of $[Mo_2S_4]^{2+}$ moieties studied by Enemark et al.[31,34] give Mo^{V}=S distances in the range 2.085–2.129 Å, averaging 2.10 for the five determinations. (Mo^{V}–S single bonds usually average 2.45 Å.) In the recently completed structure[35] of III, the Mo–S distance for the analogous terminal –SH group is nearly identical, 2.49 Å. Were it not for the strong Mo=O bond trans to the Mo—SH bond in this molecule, the Mo—SH distance would probably be a bit shorter but not, we feel, by more than 0.1 Å. It appears that the oxidation state of the Mo has relatively little effect on the Mo—S distance.

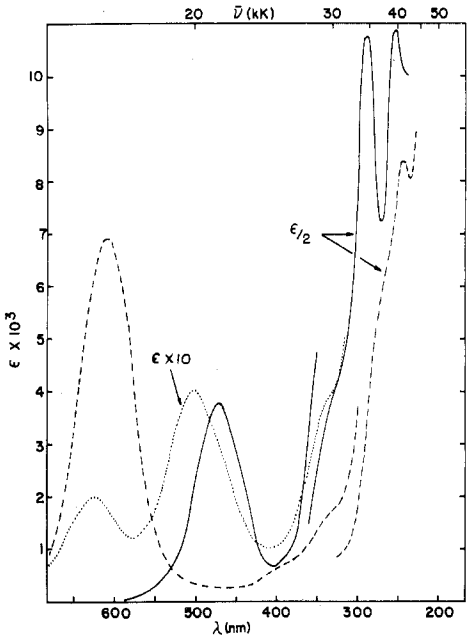

Figure 5. Optical spectra: I, —, λ_{max} 470 nm (3700), 285 nm (21 600); II, ---, λ_{max} 610 nm (6950), 240 nm (16 800); III, ···, λ_{max} 625 nm (200), 505 nm (400).

All of these points considered, we feel that the most appropriate assignment of oxidation state is Mo^{II} and that the terminal sulfur is a singly bonded hydrosulfide sulfur. To our knowledge no other Mo^{II} complex has been found to date to possess the nonbridging –SH anion. This could have interesting consequences for the reactivity of molecules of this sort.

The conformation of the ring has been previously alluded to in discussion of the consequences of the bridge. Figures 1, 2, and 4 show that the two rings are bent away from each other leaving the center of the molecule relatively exposed. This feature, too, should have interesting consequences for the reactivity of the molecule.

The dihedral angles show no unusual strain in the ring, and the vicinity of the ring surrounding the bridging sulfur is, by the usual criteria, less strained than the rest of the molecule. In this part of the ring, dihedral angles approach 60 and 180° most closely, although whether these angles are the minimum strain angles in these sulfur-containing rings is open to some question.

The anion exhibits no unusual features. The S–O distances average 1.41 Å about the tetrahedral sulfur. One of the C–F distances is a bit short, at 1.21 Å, but aside from the large thermal parameters usually associated with CF_3 groups there seems no obvious cause for this slight irregularity.

There appear to be no intermolecular contacts within 4.0 Å or evidence of extended structure in this molecule. The S(5)–S'(5) distance is 3.726 Å, far too long for any chain-like structure to exist.

The optical spectrum of I, a d^4 ion, is shown in Figure 5 where λ_{max} and $\epsilon_{\lambda max}$ are also given. The relatively high values of ϵ, at least for the 470-nm transition which is likely to be metal centered, is consistent with the distorted nature of the coordination sphere. There is nothing otherwise remarkable about this spectrum.

Likewise the IR spectrum, shown in Figure 6 in the 1500–400 cm^{-1} range, is unremarkable. Most of the spectral

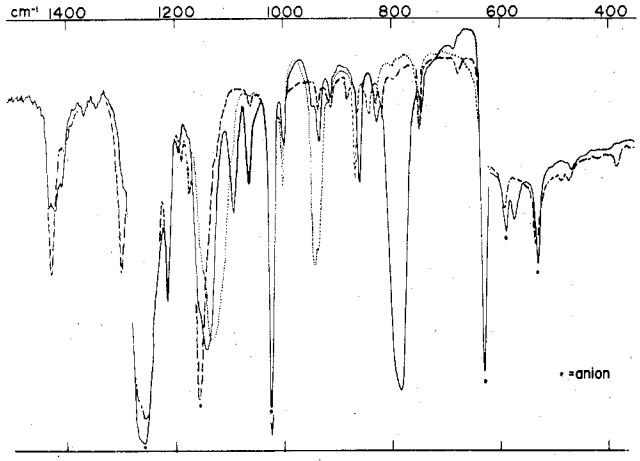

Figure 6. Infrared spectra: I, ---; II, —; III, ···.

range is obscured by intense anion absorption. The absence of the strong Mo–O stretches found in II and III is indicative of the purity of the complex. IR would offer the best opportunity for detection of the –SH stretch in the region 2200–2500 cm^{-1}. However it appears that this absorption, if it exists, is either very broad and weak or shifted to some other part of the spectrum where it is not readily identified.

The question of whether I retains its conformation in solution is resolved by consideration of the symmetry of the complexed macrocycle relative to the free. The free macrocycle contains two sets of inequivalent protons which in the ^1H NMR give rise to a pentuplet and a triplet in a 1:2 intensity ratio. Coordination in the manner observed in I leads to a mirror of symmetry bisecting the ring. The proton NMR is exceedingly complex. ^{13}C NMR, however, would be expected to show six inequivalent carbon resonances relative to two in the free ligand. Figure 7 shows that this is indeed observed. Thus we may conclude that I retains its solid-state structure in solution. Assignment of the resonances has not been attempted, although one may safely assume that those shifted furthest downfield belong to carbons nearest the sulfur.

Electrochemical studies are one means by which we hope to study in detail the electronic structure of this complex. We report here preliminary cyclic voltammetric measurements (Figure 8). Working in CH_3CN solution we see that I undergoes a pseudo-reversible one-electron redox process, presumably between Mo^{II} and Mo^{I}. Reduction occurs at ca. –1.0 V vs. aqueous SCE, and reoxidation at ca. –0.9 V. The Mo^{I} species produced is thus about as good a reducing agent at Cr^{2+}. If the species produced is indeed Mo^{I}, this d^5 species should be amenable to ESR analysis leading to (1) unambiguous characterization as Mo^{I} and (2) an estimate of the extent of metal–metal interaction if any. Studies are underway aimed at answering these questions.

$[Mo_2^{IV}O_2(16\text{-ane}[S_4])_2OC_2H_5](CF_3SO_3)_3$ (II). This complex (Figure 1(ii)) is the least stable of the three complexes under discussion. The solid seems indefinitely stable when stored in a capped vial, but solutions are much less so. Aqueous solutions quickly turn pale violet and then colorless, while in CH_3CN, the bright blue color is retained for several days. One can perhaps understand this relative instability by considering the structure. Reaction with water and/or solvent ethanol has resulted in a dimer Mo^{IV}=O species held together *solely* by the relatively long and presumably weak, single oxo bridge. Mo^{IV}=O distances are both 1.76 Å, while the bridging oxygen–molybdenum bond distance is 2.14 Å, and the molybdenum–ethoxide oxygen single bond distance is 1.86 Å.[36] Other structural features worth pointing out are the out-of-plane distances of the molybdenum atoms: 0.33 Å for the "upper" ring and –0.10 Å for the "lower" ring where Mo is coordinated fairly strongly to –OEt and the staggering of the two macrocyclic rings at an angle of 43°. The distance between the two Mo atoms of the dimer is 3.90 Å. Ring conformation is fairly regular and free of metal-imposed strain.[25]

The optical spectra shown in Figure 5 show considerably higher ϵ in the visible region than found in I, again presumably

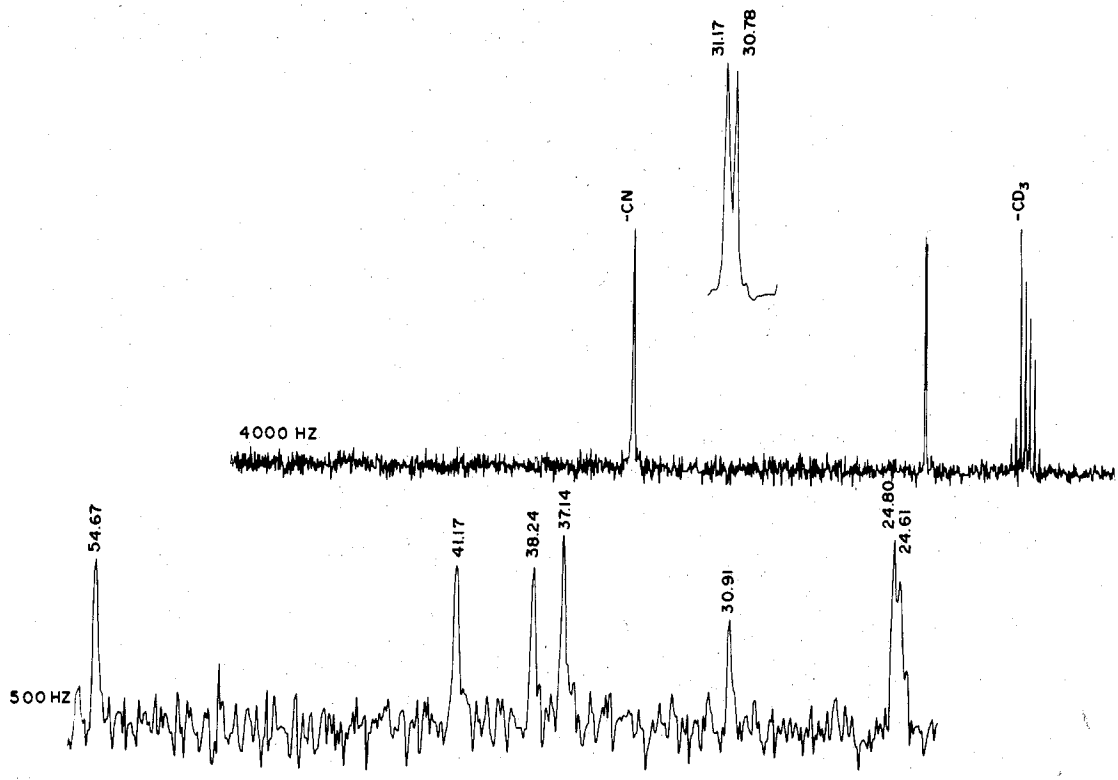

Figure 7. ^{13}C NMR of I: upper trace, free ligand; lower trace, complex.

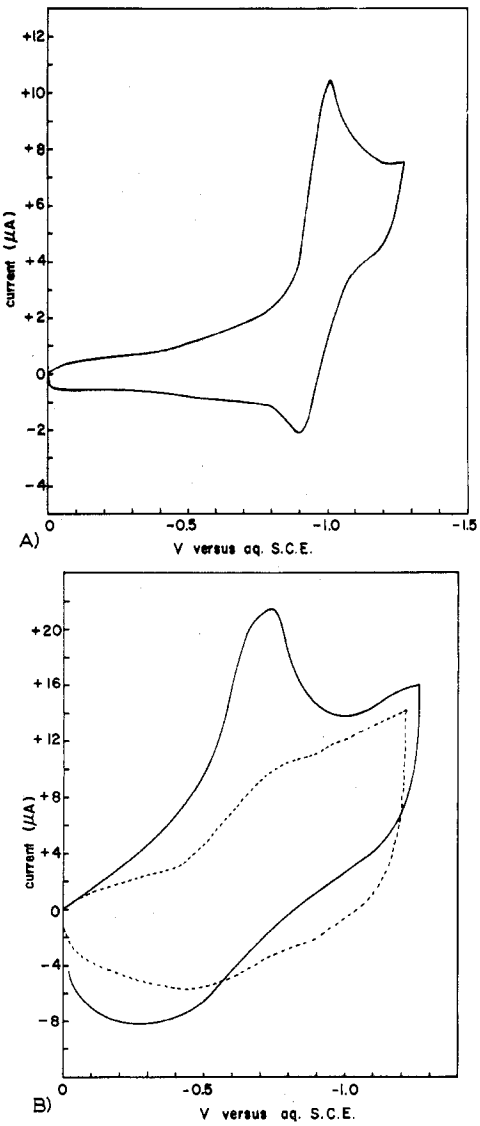

Figure 8. Cyclic voltammograms: (A) I; (B) II, —; III, ---.

due to the strong axial component to the ligand field, associated with the Mo=O moiety. As expected for Mo^{IV} in this ligand field, II is diamagnetic.

As with I, the infrared spectrum is substantially obscured by intense anion bands, but the features due to the Mo–O coordination stand out clearly. Terminal Mo=O stretches usually occur in the 920–1000-cm^{-1} range while bridging Mo–O–Mo stretches are found in the vicinity of 800 cm^{-1}. Both of these modes usually give rise to rather intense IR absorption. The relatively weak absorption at ~960 cm^{-1} and the very strong absorption at ~780 cm^{-1} would tend to indicate that the entire O=Mo···O=Mo—O– unit is fairly strongly coupled. A weak coupling would allow both Mo=O moieties to vibrate as essentially terminal oxomolybdenum units which is clearly not the case here.

Cyclic voltammetry in CH_3CN shows the redox process undergone by II to be irreversible. Reduction occurs at ca. –0.7 V with the production of uncharacterized species, among them probably the monomeric cleavage products. It seems reasonable that addition of an electron to the metal ion would reduce the strength of the already weak bridging interaction—on acid–base grounds alone—and promote dissociation of the complex. One of the cleavage products would be five-coordinate and could readily react with solvent or other reactive species present. The chances of recombination to form the original complex would be rather slim. A further electrochemical ESR study should reveal more about the nature of the reduced species.

[MoO(SH)(16-ane[S_4])](CF_3SO_3) (III). The only monomeric complex isolated in this study is presumably formed by decomposition of I, under conditions similar to those which yield II. Coordinated –SH could have originated only via I since the complex did not appear for several days, during which time solvent attack on I remaining in solution could have occurred. Like I and II, III is diamagnetic and, formulated with a terminal –SH group, requires molybdenum to be in the +4 oxidation state. Comments of a crystallographic nature made about the –SH group in I apply equally to III. The Mo–S(terminal) bond length is 2.49 Å, just about the same as in I. Based on Mo^{IV} vs. Mo^{II}, the distance would be expected to be shorter in III than in I, but the strong Mo=O bond in III probably results in a weaker and longer trans bond to S. Mo–S(ring) bonds average 2.47 Å and the Mo ion sits 0.07 Å out of the plane, displaced toward the oxygen.[35] This nonplanarity is quite small and is probably due more to the unequal strength of the two axial ligands than any factors involving cavity size.

The optical spectrum of III, Figure 5, shows extinction coefficients an order of magnitude lower than observed for I and II in the visible region of the spectrum, and is much more typical of "normal" metal complexes with less distorted geometries. The IR spectrum (Figure 6) shows clearly the terminal M=O stretch at 960 cm^{-1}; no other features of note are apparent.

Cyclic voltammetry shows this complex to undergo an irreversible redox process as does II. In view of the simplicity of the molecule, it is not clear why reduction should be irreversible. No obviously unstable species is produced upon the addition of one electron. Just what is happening in this electrochemical process will have to be determined by a much more thorough study including consideration of electrode surface effects.

In summary, this work has significantly expanded our knowledge of the behavior of cyclic polythiaethers and their complexes. New complexes exhibiting a range of oxidation states and geometries have been produced. Complete structural characterization has provided us with necessary knowledge needed for future in-depth studies of bonding in these systems. Hopefully this work can be extended to other similar ring systems in order to more fully detail the effects of macrocycle size on complex formation and properties.

Acknowledgment. Acknowledgment is made to the donors of the Petroleum Research Fund, administered by the American Chemical Society, for support of this research. We also acknowledge the National Science Foundation (Grants CHE75-17217 and CHE77-02664 A01) and thank Dr. Ronald Schroeder and Dr. William Sokol for help with the electrochemical measurements and Dr. Edwin Abbott for very helpful discussions.

Registry No. I, 67351-06-8; II, 67351-08-0; III, 67351-10-4; ^{13}C, 14762-74-4; $Mo_2(O_2CH)_4$, 51329-49-8.

Supplementary Material Available: A listing of calculated and observed structure factors and a stereoscopic view of the unit cell contents (13 pages). Ordering information is given on any current masthead page.

References and Notes

(1) N. F. Curtis, *Coord. Chem. Ref.*, **3**, 3 (1968).
(2) L. F. Lindoy and D. H. Busch, *Prep. Inorg. React.*, **6**, 1 (1971).
(3) J. E. Baldwin et al., *J. Am. Chem. Soc.*, **97**, 226 (1975).
(4) J. P. Collman et al., *J. Am. Chem. Soc.*, **97**, 1427 (1975).
(5) D. G. Pillsbury and D. H. Busch, *J. Am. Chem. Soc.*, **98**, 7836 (1976).
(6) C. J. Pederson and H. K. Frensdorff, *Angew. Chem., Int. Ed. Engl.*, **11**, 6 (1972).
(7) J. D. Dunitz and P. Seiler, *Acta Crystallogr., Sect. B*, **30**, 2739 (1974).
(8) J.-M. Lehn, *Struct. Bonding (Berlin)*, **16**, 1 (1973).
(9) W. Rosen and D. H. Busch, *Inorg. Chem.*, **9**, 262 (1970).

(10) K. Travis and D. H. Busch, *Inorg. Chem.*, **13**, 2591 (1974).
(11) E. R. Dockal, L. L. Diaddario, M. D. Glick, and D. B. Rorabacher, *J. Am. Chem. Soc.*, **99**, 4530 (1977).
(12) T. E. Jones, L. L. Zimmer, L. L. Diaddario, D. B. Rorabacher, and L. A. Ochrymowycz, *J. Am. Chem. Soc.*, **97**, 7163 (1975).
(13) P. H. Davis, L. K. White, and R. L. Belford, *Inorg. Chem.*, **14**, 1753 (1975).
(14) J. T. Spence, *Coord. Chem. Rev.*, **4**, 475 (1969).
(15) W. G. Zumft and L. E. Mortenson, *Biochim. Biophys. Acta*, **416** 1 (1975).
(16) R. C. Bray and J. C. Swann, *Struct. Bonding (Berlin)*, **11**, 107 (1972).
(17) L. A. Ochrymowycz, C. P. Mak, and J. D. Michna, *J. Org. Chem.*, **39**, 2079 (1974).
(18) T. Tighe and R. E. DeSimone, *J. Inorg. Nucl. Chem.*, **38**, 1623 (1976).
(19) R. E. DeSimone, unpublished results.
(20) (a) R. E. DeSimone and M. D. Glick, *J. Am. Chem. Soc.*, **97**, 942 (1975); (b) R. E. DeSimone and M. D. Glick, *J. Coord. Chem.*, **5**, 181 (1976).
(21) R. E. DeSimone and M. D. Glick, *J. Am. Chem. Soc.*, **98**, 762 (1976).
(22) E. H. Abbott, F. Schoenenolf, Jr., and T. Backstrom, *J. Coord. Chem.*, **3**, 255 (1974).
(23) We have chosen at this point to adopt the commonly used nomenclature of Busch.
(24) F. A. Cotton et al., *J. Coord. Chem.*, **5**, 217 (1976).
(25) (a) Local versions of the following programs were used: (1) TRACER II, S. L. Lawton's cell reduction program; (2) SYNCOR, W. Schmonsees' program for data reduction; (3) NEWES, W. Schmonsees' program for generation of normalized structure factors; (5) FORDAP, A. Zalkin's Fourier program; (6) ORFLS and ORFFE, W. Busing, K. Martin, and H. Levy's full-matrix least-squares program and function and error program; (7) H-FINDR, A. Zalkin's program for H-atom positions; (8) ORTEP, C. K. Johnson's program for drawing crystal models. (b) Neutral atom scattering factors for Mo, S, F, O, C, and H were taken from "The International Tables for X-Ray Crystallography", Vol. IV, J. A. Ibers and W. C. Hamilton, Ed., The Kynoch Press, Birmingham England, 1974.
(26) R. E. DeSimone, unpublished observations.
(27) See paragraph at end of paper regarding supplementary material.
(28) B. Spivak, Z. Dori, and E. I. Stiefel, *Inorg. Nucl. Chem. Lett.*, **11**, 501 (1975).
(29) M. G. B. Drew and A. Kay, *J. Chem. Soc. A*, 1851 (1971).
(30) D. H. Brown and J. A. B. Jeffreys, *J. Chem. Soc., Dalton Trans.*, 732 (1973).
(31) G. Bunzey and J. H. Enemark, *Inorg. Chem.*, **17**, 682 (1978).
(32) B. Spivak, A. P. Gaughan, and Z. Dori, *J. Am. Chem. Soc.*, **93**, 5265 (1971).
(33) L. A. Ochrymowycz, personal communication.
(34) J. T. Huneke and J. H. Enemark, *Inorg. Chem.*, in press.
(35) R. E. DeSimone and M. D. Glick, *Inorg. Chem.*, in press.
(36) R. E. DeSimone, J. Cragel, Jr., W. H. Ilsley, and M. D. Glick, *J. Coord. Chem.*, in press.

Contribution from the Department of Chemistry, University of Oklahoma, Norman, Oklahoma 73019

Crystal and Molecular Structures of Two Molybdenum Complexes with Tetraphenylborate As a π-Bonding Ligand: (I) Cycloheptatrienyl(tetraphenylborato)molybdenum and (II) Tetraethylammonium Tricarbonyl(tetraphenylborato)molybdate

M. BILAYET HOSSAIN and DICK VAN DER HELM*

Received February 3, 1978

The crystal and molecular structures of (I) cycloheptatrienyl(tetraphenylborato)molybdenum, $Mo(\eta^7\text{-}C_7H_7)(\eta^6\text{-}C_6H_5B(C_6H_5)_3)$, and (II) tetraethylammonium tricarbonyl(tetraphenylborato)molybdate, $[(C_2H_5)_4N][Mo(CO)_3(\eta^6\text{-}C_6H_5B(C_6H_5)_3)]$ have been determined from three-dimensional X-ray diffraction data. The compounds crystallize in the triclinic space group $P\bar{1}$ with the following crystal data. Complex I: $a = 9.93$ (1) Å, $b = 11.15$ (1) Å, $c = 10.92$ (1) Å, $\alpha = 97.6$ (1)°, $\beta = 90.4$ (1)°, $\gamma = 106.1$ (1)°, $V = 1150$ (4) Å^3, $Z = 2$, $D_x = 1.461$ g cm^{-3}. Complex II: $a = 10.58$ (1) Å, $b = 12.454$ (8) Å, $c = 11.831$ (7) Å, $\alpha = 101.32$ (5)°, $\beta = 96.88$ (7)°, $\gamma = 90.59$ (7)°, $V = 1517$ (4) Å^3, $Z = 2$, $D_x = 1.378$ g cm^{-3}. In each case intensity data were collected at -135 ± 2 °C on an automatic diffractometer using zirconium-filtered Mo radiation. Both structures were solved by the heavy-atom method and refined by least-squares techniques. The final R value for all 4737 reflections of complex I is 0.063, and for the 6246 reflections of complex II it is 0.066. In compound I, the molybdenum atom is sandwiched between, and directly bonded to, a cycloheptatrienyl ring and one of the phenyl rings of the BPh_4 group. Mo–C distances for the C_7H_7 ring are considerably shorter (average value 2.274 Å) than the corresponding distances for the phenyl ring. In both complexes, the distance of the metal to ring carbon bonded to the boron atom is significantly longer (0.089 Å in complex I and 0.060 Å in complex II) than the average of the rest of the five Mo–C(phenyl) distances (2.341 Å in complex I and 2.372 Å in complex II). All C–H bonds in the two rings forming the sandwich in complex I are significantly bent toward the metal atom. In complex II, the phenyl ring and the three carbonyl ligands form a near-staggered geometry around the molybdenum. In this complex, part of the tetraethylammonium group was found to be disordered.

Introduction

The two molybdenum complexes under investigation, $Mo(\eta^7\text{-}C_7H_7)(\eta^6\text{-}C_6H_5B(C_6H_5)_3)$—complex I—and $[(C_2H_5)_4\text{-}N][Mo(CO)_3(\eta^6\text{-}C_6H_5B(C_6H_5)_3)]$—complex II—were prepared[1] as a part of a program to synthesize and characterize derivatives of the transition metals with tetraphenylborate as a π-bonding ligand and to study the feasibility of using these compounds as oxidation–reduction catalysts. Structural features of metal–arene complexes, particularly the distortion of arene rings by π complexation, have drawn wide attention.[2-5] Although there are several structure reports of molybdenum complexes with η^5-cyclopentadienyl[6-9] and η^7-cycloheptatrienyl[10-12] ligands, complexes of benzene or benzene derivatives with molybdenum are rare.[13] Complex I, which shows a remarkable number of oxidation states (it undergoes three reversible oxidation–reduction reactions,[1] is the only reported sandwich structure of molybdenum with an η^7-C_7H_7 ligand and a phenyl ring. The structural details of such a sandwich complex would be helpful in understanding the dependence of metal-to-ring atom distance on the size of the ring.

Experimental Section

Crystal Data. The crystals of the two compounds were kindly supplied to us by Dr. D. A. Owen of the University of Oklahoma.

The crystals of complex I are fairly well-developed plates. The deep green crystals get a dark dusty coating after several days of

0020-1669/78/1317-2893$01.00/0